fermentation

MDPI

Article

Degradation of Anti-Nutritional Factors in Maize Gluten Feed by Fermentation with *Bacillus subtilis*: A Focused Study on Optimizing Fermentation Conditions

Xiaohong Sun [1,2], Lei Ma [2], Yaoquan Xuan [1] and Jianfen Liang [2,*]

[1] School of Food and Pharmacy, Zhejiang Ocean University, Zhoushan 316022, China; sunxh@zjou.edu.cn (X.S.); 15757295882@163.com (Y.X.)
[2] College of Food Science and Nutritional Engineering, China Agricultural University, Beijing 100083, China; malei7456@163.com
* Correspondence: liangjf@cau.edu.cn; Tel.: +86-010-62737699

Abstract: Maize gluten feed is rich in micronutrients and serves as a good source of protein and dietary fiber, but also contains anti-nutritional factors. In this study, fermentation conditions for the degradation of phytic acid and water-unextractable arabinoxylans in maize gluten feed using *Bacillus subtilis* were optimized. Key variables influencing the fermentation process were identified from seven potential parameters using the Plackett–Burman design. Three statistically significant factors, i.e., fermentation time, inoculum dose, and material-to-liquid ratio were further optimized through a central composite design and the efficiency of fermentation conditions was predicted. The accuracy of the predicted model was validated by subsequent experimentation. The optimum fermentation conditions were determined to be a fermentation time of 84.5 h, inoculum dose of 17.1%, and material-to-liquid ratio of 1:3.4. Under these conditions, 48% of phytic acid and 32% water-unextractable arabinoxylans were degraded. Following fermentation, the activities of protease, xylanase, phytase, and cellulase in maize gluten feed were significantly increased ($p < 0.001$), contributing to the breakdown of phytic acid and water-unextractable arabinoxylans, which improved the protein dispersibility index, in vitro protein digestibility, and mineral bioavailability. These findings suggest that fermenting maize gluten feed with *Bacillus subtilis* is a practical and effective approach to reducing anti-nutrients and enhancing its nutritional quality.

Keywords: maize gluten feed; phytic acid; water-unextractable arabinoxylans; *Bacillus subtilis*; fermentation; in vitro protein digestibility; minerals

Citation: Sun, X.; Ma, L.; Xuan, Y.; Liang, J. Degradation of Anti-Nutritional Factors in Maize Gluten Feed by Fermentation with *Bacillus subtilis*: A Focused Study on Optimizing Fermentation Conditions. *Fermentation* **2024**, *10*, 555. https://doi.org/10.3390/fermentation10110555

Academic Editors: Mohamed Koubaa and Spiros Paramithiotis

Received: 19 September 2024
Revised: 11 October 2024
Accepted: 27 October 2024
Published: 31 October 2024

1. Introduction

Maize (*Zea mays*), a monocotyledon of the Gramineae family, is one of the major cereal grains cultivated all over the world. Maize gluten feed (MGF), a by-product of the wet-milling process used for starch (or ethanol) production, is primarily composed of germ meal, bran, and dried steep liquor [1]. MGF contains 20–28% protein, and protein from maize germ offers a favorable balance of the essential amino acids and high biological value [2,3]. In addition to its protein content, MGF is rich in dietary fiber, which has entered the limelight as a potential high dietary fiber food ingredient. It also contains significant levels of carotenoids, polyphenols, and other bioactive compounds [4,5]. However, the utilization of MGF in food products is limited due to the existence of anti-nutrients, mycotoxins, and its adverse effects on textures and flavors. Our present study is primarily focusing on addressing the anti-nutritional substances in MGF.

Phytic acid (PA) and arabinoxylans are two of the primary anti-nutritional substances in MGF. Normally, PA predominantly exists in cereal grains in form of phytate, where it forms covalent bonds with mineral cations, such as calcium, iron, and zinc. This binding reduces the bioavailability of these essential minerals and decreases the digestibility of

protein and starch in the digestive tract [6,7]. Approximately 80% of the PA in maize is concentrated in the germ [8], which is transferred into MGF during germ processing. Previous studies had shown that MGF contains 11.4 ± 0.2 mg/g of phosphorus, significantly higher than the 2.6 ± 0.2 mg/g found in maize, with most of the phosphorus present as phytate [8,9]. In addition to PA, MGF is also rich in non-starch polysaccharides, particularly arabinoxylans [1]. Studies on wheat by-products have demonstrated that arabinoxylans can reduce nutrient digestibility [10]. Arabinoxylans contain a linear backbone of β-(1–4)-linked D-xylopyranosyl and with α-L-arabinofuranose as the side chains [11]. The majority of arabinoxylans in MGF are water-unextractable arabinoxylans (WU-AXs), which are more resistant to digestion [12]. The anti-nutritional effects of WU-AXs are attributed to their binding within cell walls by covalent or non-covalent interactions with other nutrients, making them inaccessible to the digestive system [13,14].

Anti-nutritional substances in cereals and their co-products can be decreased through various processing techniques, including physical, chemical, and biological proccessing techniques [15]. Among these, fermentation, one of the oldest and most efficient techniques, is widely used in food production to improve nutritional quality by leveraging microbial activity. *Bacillus subtilis*, Gram-positive aerobic bacteria, is categorized as Generally Recognized as Safe (GRAS) by the FDA [16]. It commonly used in diverse Asian traditional fermentation food owing to its ability to produce considerable amounts of dissimilar enzymes such as proteases, phytase, and cellulase [17]. Previously studies have shown that exogenous xylanases can break down long WU-AX backbones into smaller fragments, enhancing nutrient absorption and generating arabinoxylooligosaccharides with prebiotic effects [13]. Studies have also reported that *Bacillus* species could reduce the level of anti-nutritional factors and enhance the nutritional value of soybean products [18]. While there has been considerable research into the use of exogenous enzymes to reduce anti-nutritional factors, fewer studies have explored the full potential of microbial fermentation, particularly using *Bacillus subtilis*, for this purpose in MGF. Our study is novel in that it focuses on optimizing the fermentation process to simultaneously target the degradation of both PA and WU-AX in MGF, offering a more integrated and sustainable approach compared to chemical or enzyme-only treatments.

Aiming at decreasing anti-nutrients, the fermentation of MGF with *Bacillus subtilis* was carried out to establish optimal fermentation parameters for the degradation of PA and WU-AX simultaneously. In this study, Plackett–Burman design (PBD) and central composite design (CCD) were employed to optimize the fermentation conditions. Plackett–Burman design efficiently screens and identifies key factors, while central composite design, a response-surface methodology (RSM), is one of the most effective tools for process optimization. The combination of Plackett–Burman design and central composite design has been reported in many process optimizations [19]. This work proposes a relatively simple processing technology to decrease anti-nutrients in maize processing co-products with potential applications in the food manufacturing industry.

2. Materials and Methods

2.1. Sample Preparation

Maize gluten feed (MGF) was obtained from Cargill Biochemical Co., Ltd. (Songyuan, China), containing 27.13% protein (N × 6.25), 11% moisture, 9% ash, and 2% fat. The plant material was milled using a universal high-speed crusher (150 T, Yongkang Boou Hardware Products Co., Ltd., Jinhua, China) and passed through sieves with mesh sizes of 18, 40, 80, 140, and 200. As a result, MGF samples with mean particle sizes of 585, 189, 123, 30, and 14 μm, respectively, were obtained.

Bacillus subtilis (CICC 24602) was obtained from the China Center of Industrial Culture Collection (CICC, Beijing, China). *Bacillus subtilis* (CICC 24602), isolated from Baijiu Daqu, has been shown to secrete various enzymes, including saccharifying enzyme, protease, amylase, cellulase, and phytase. The freeze-dried powder was cultured on a medium (peptone 5.0 g, beef extract 3.0 g, NaCl 5.0 g, agar 15.0 g, distilled water 1.0 L, pH 7.0) for

activation and propagation, following the method provided by the CICC. A seed culture was prepared by inoculating a single loop of *Bacillus subtilis* into 50 mL of sterile medium (peptone 5.0 g, beef extract 3.0 g, and NaCl 5.0 g, distilled water 1.0 L, pH 7.0) in a 250 mL flask and incubating at 37 °C for 8 h with shaking at 150 rpm (shaker incubator THZ-98c, Shanghai Bluepard Experimental Instrument Co., Ltd., Shanghai, China). The resulting seed culture, containing approximately 10^8 cfu/mL, was used for MGF fermentation.

2.2. Fermentation of Maize Gluten Feed

Weighed MGF samples were placed into 380 mL glass containers ($7 \times 7 \times 8$ cm^3, with a circular opening diameter of 6 cm), covered with breathable sealing film to allow air exchange, and then autoclaved at 121 °C for 20 min (Panasonic MLS-3751L-PC, Kadoma, Japan). After cooling to room temperature, the samples were inoculated with the seed culture, supplemented with a specific volume of sterile water, and thoroughly mixed under sterile conditions in an ultra-clean workbench. The containers were then incubated in a biochemical incubator (LHS-HC-I, Shanghai Bluepard Experimental Instrument Co., Ltd., Shanghai, China). After a designated fermentation period, the fermented MGF was vacuum freeze-dried, followed by milling and sieving through an 80-mesh screen.

2.3. Determination of Phytic Acid

The PA content was determined according to the method described by Buddrick et al. [20]. Briefly, PA was extracted with 0.2 mol/L hydrochloric acid and precipitated with a ferric chloride solution of known iron concentration. The decrease in iron in the supernatant is taken as a measure of phytic acid content. Absorbance was recorded at 519 nm, and the method was calibrated using reference solutions prepared by diluting a stock solution with 0.2 mol/L HCl, yielding PA concentrations ranging from 0.13 to 1.3 mg/mL.

2.4. Determination of Water-Unextractable Arabinoxylan

The determination of arabinoxylans was carried out following the methods described by Douglas [21] and Rouau and Surget [22], with some modification. The concentration of WU-AX was calculated by subtracting the water-extractable arabinoxylan (WE-AX) content from the concentration of total AX. Briefly, WE-AX was extracted by dispersing the sample in distilled water (10% w/v) and shaking at 4 °C (cold extraction). For total AX extraction, the sample was treated with 1 mol/L sulfuric acid (10% w/v) and boiled for 2.5 h. After cooling to room temperature, the sample was neutralized with 2 mol/L sodium carbonate. The arabinoxylans content in both extracts was quantified using the phloroglucinol colorimetric assay, following the method described by Hernán-dez-Espinosa et al. [23], with some modification based on the original protocol proposed by Rouau and Surget [22].

2.5. Optimization Experimental Design

Fermentation conditions were optimized using PA and WU-AX content as indicators. The optimization process involved three steps: (1) a single-factor test to establish the appropriate range for each factor, (2) the Plackett–Burman design to identify key factors influencing the fermentation process, and (3) further optimization of key variables using a central composite design.

2.5.1. Single-Factor Test

Seven factors were considered in the single-factor experiments, including fermentation time, temperature, initial pH, inoculum dose, particle size, substrate filling rate, and material-to-liquid ratio. In each test, one factor was varied while the other six factors were kept constant at their baseline levels. The baseline conditions for the seven factors were as follows: fermentation time of 72 h, temperature of 37 °C, initial pH of 6.5, inoculum concentration of 10%, particle size of 123 μm, substrate filling rate of 3.43%, and a material-

to-liquid ratio of 1:2. Six different fermentation durations were set at 24, 48, 72, 96, 120, and 144 h. Six fermentation temperatures were tested at 25, 28, 31, 34, 37, and 40 °C. Seven initial pH levels were adjusted to 5.0, 5.5, 6.0, 6.5, 7.0, 7.5, and 8.0. Maize germ meal was milled for different durations using a high-speed grinder and then passed through sieves with mesh sizes of 18, 40, 80, 140, and 200, resulting in average particle sizes of 585, 189, 123, 30, and 14 μm, respectively. Six different substrate filling rates were set at 4, 7, 10, 13, 16, and 19 g, corresponding to 1.05%, 1.84%, 2.63%, 3.42%, 4.21%, and 5.00% of the total volume of the fermentation vessel, respectively. Seven material-to-water ratios were tested: 1:1, 1:1.5, 1:2, 1:2.5, 1:3, 1:3.5, and 1:4. Additionally, six inoculation levels were used: 5%, 10%, 15%, 20%, 25%, and 30%. Each treatment in the single-factor experiments was repeated three times, and the average value was reported as the experimental result.

2.5.2. Plackett–Burman Design

Plackett–Burman design was employed to assess the relative significance of the seven factors on the content of PA (Y_1) and WU-AX (Y_2), thereby identifying the key independent variables for further optimization. Based on the results of the single-factor tests (Supplementary Table S1), the seven factors were evaluated at two levels: low (−1) and high (+1). The design involved 12 experimental runs, each with a different combination of factor levels, along with a 13th run under baseline conditions. All experiments were performed in triplicate, and the mean PA and WU-AX contents in the fermented samples were recorded as the dependent variables (responses). A first-order polynomial model was applied to fit the Plackett–Burman design, assuming no interactions between variables, as shown in Formula (1).

$$Y = \beta_0 + \sum_{i=1}^{7} \beta_i X_i \quad (1)$$

where Y represents the predicted response, β_0 denotes the intercept, β_i corresponds to the linear regression coefficient, and X_i refers to the coded independent variable.

Factors with confidence levels exceeding 95% ($p \leq 0.05$) were considered to have a statistically significant effect on the degradation of PA and WU-AX and were selected for further optimization.

2.5.3. Central Composite Design

In the central composite design, three factors—fermentation time (hour), inoculum dose (%, *v*/*w*), and the material-to-liquid ratio—denoted as X_1, X_4, and X_7 respectively, were selected from the Plackett–Burman design for further factorial optimization. Each variable was tested at five coded levels ($-\alpha$, -1, 0, +1, $+\alpha$, with $\alpha = 2$), while the remaining factors from the Plackett–Burman design were held at their optimal levels. A total of 19 experimental runs were designed, including 5 replicates at the central point, with all runs performed in triplicate. The degradation of anti-nutritional substances was analyzed using a second-order polynomial equation, and the data were fitted through a multiple regression procedure. The mathematical relationship between the response variables Y_1 (PA content) and Y_2 (WU-AX content) and the significant independent variables X_1, X_4, and X_7 was expressed by the following quadratic polynomial equation (Formula (2)):

$$Y = \beta_0 + \sum_{i=1}^{3} \beta_i X_i + \sum_{i=1}^{3} \beta_{ii} X_i^2 + \sum_{i=1}^{2} \sum_{j=i+1}^{3} \beta_{ij} X_i X_j \quad (2)$$

where Y is the response, the contents of PA (Y_1) and the contents of WU-AX (Y_2); β_0 is the constant coefficient, β_i represents the linear coefficients, β_{ii} represents the quadratic coefficients, β_{ij} represents the interaction coefficients, and X_i and X_j are the coded values of the independent variables.

The fitted polynomial equation was expressed as a surface in order to visualize the relationship between the response and experimental levels of each factor and to deduce the optimum conditions. The analysis of the experimental design and calculation of predicted data were carried out using Design Expert software Version 8.0.6.1 (Stat-Ease, Inc.,

Minneapolis, MN, USA) to estimate the response of the independent variables. Subsequently, three additional validation experiments were conducted to verify the validity of the statistical experimental strategies.

2.6. Enzymatic Activity Analysis

2.6.1. Phytase Activity Assay

Phytase activity was determined based on the ammonium vanadate-molybdate method [24]. Phytase catalyzes the hydrolysis of phytate, generating orthophosphate and inositol derivatives. The released orthophosphate reacts with ammonium vanadate-molybdate under acidic conditions to form a yellow phosphomolybdic acid complex, which is quantified colorimetrically at 415 nm. One unit of phytase activity (U) was defined as the amount of enzyme required to released 1 μmol inorganic phosphorus per minute from a 5 mmol/L sodium phytate substrate under the specified assay conditions.

2.6.2. Xylanase Activity Assay

Xylanase activity was quantified using the 3,5-dintrosalicylic acid (DNS) assay for reducing sugars, following the method outlined by Dhaver et al. [25]. Xylanase catalyzes the degradation of xylan into reducing oligosaccharides and monosaccharides, which subsequently react with DNS under boiling conditions. The resulting colorimetric reaction produces an absorption peak at 540 nm. One unit of xylanase activity (U) was defined as the amount of enzyme required to release 1 μmol of reducing sugars per minute from a 5 mg/mL xylan solution under the specified assay conditions.

2.6.3. Cellulase Activity Assay

Cellulase activity was measured by quantifying the reducing sugars released during hydrolysis, using the DNS method [26]. Cellulase hydrolyzes filter paper strips (1 × 6 cm), producing reducing sugars such as cellobiose and glucose. These sugars react with DNS under alkaline conditions, forming a reddish-brown compound. One unit of cellulase activity (U) was defined as the amount of enzyme required to release 1 μmol of glucose per minute from the filter paper under the specified assay conditions.

2.6.4. Protease Activity Assay

Protease activity was determined using the Folin–Ciocalteu's phenol reagent method following the method described by Wang et al. [27]. Briefly, an appropriately diluted enzyme sample was added to a casein solution, and the reaction was terminated by the addition of 10% trichloroacetic acid. After centrifugation, the absorbance of the supernatant was measured at 680 nm to quantify the amount of tyrosine released. A standard curve was generated using tyrosine (5–50 μg/mL). One unit of protease activity (U) was defined as the amount of enzyme required to release 1 μg of tyrosine per minute from casein under the specified assay conditions.

2.7. Protein Nutritional Analysis

The protein dispersibility index (PDI) was determined following the method described by Zhang et al. [28]. In this procedure, 0.5 g of the sample was dissolved in 20 mL of deionized water and stirred at 500 r/min for 1 h. The mixture was then centrifuged at 10,000× *g* for 20 min, after which the total protein content in the supernatant and the original sample was quantified using the Kjeldahl method. PDI was calculated using the following formula (Formula (3)):

$$\text{PDI} = \frac{\text{The protein content in supernatant}}{\text{Total protein content in sample}} \times 100 \quad (3)$$

The degree of hydrolysis (DH) is defined as the percentage of free amino groups cleaved from protein and was calculated from ratio of free amino nitrogen of hydrolysate amino nitrogen and total nitrogen [28]. DH was determined using the ninhydrin colorimet-

ric method, as described by Pearce, Karahalios, and Friedman [29]. A standard curve was generated using glycine as the amino acid standard, with absorbance readings at 570 nm. DH was calculated using the following formula (Formula (4)):

$$\text{DH} = \frac{\text{Free amino nitrogen of sample}}{\text{Total nitrogen in sample}} \times 100 \quad (4)$$

In vitro protein digestion (IVPD) was performed following Kamble et al. [30] with modifications. Briefly, a 1.0 g sample was incubated with 10 mL of pepsin solution (20 mg/mL, pH 2.0) at 37 °C with shaking at 190 r/min for 3 h. Subsequently, 2.0 mL of 0.5 mol/L NaOH and 30 mL of trypsin solution (5 mg/mL, pH 8.0) were added, and the mixture was shaken at 37 °C for 2 h. After centrifugation, 10 mL of 10% trichloroacetic acid was added to the supernatant, followed by a 1-h incubation and centrifugation. The protein content was determined using the Kjeldahl method. The in vitro digestion rate of the protein was calculated using the following formula (Formula (5)):

$$\text{IVPD} = \frac{\text{Nitrogenin sample} - \text{Nitrogen in residue}}{\text{Nitrogenin sample}} \times 100 \quad (5)$$

2.8. In Vitro Minerals Digestion

The in vitro mineral digestion rate was evaluated following the method of Kumar et al. [31], with modifications. A 5.0 g sample was mixed with 30 mL distilled water and shaken at 150 rpm for 2 h at room temperature. After adding 2 mL of α-amylase solution (6.25 g/L), the mixture was incubated at 37 °C for 30 min. The pH was then adjusted to 4.0 with 1 mol/L HCl, followed by the addition of 8 mL pepsin (0.125 g/L), and further incubation at 37 °C for 1 h. The pH was adjusted to 6.0 with 1 mol/L $NaHCO_3$, followed by the addition of 10 mL pancreatin solution (20 g/L), and incubated at 37 °C for 30 min. The mixture was centrifuged at 10,000 r/min for 10 min at 4 °C, and the supernatant was filtered through a 0.45 μm filter. The mineral contents (Fe, Mn, Cu, Zn) in the filtrate and samples were analyzed by ICP-OES. Mineral bioavailability was calculated using formula (Formula (6)).

$$\text{In vitro digestion of minerals}' \text{ bioavailability} = \frac{\text{Minerals in digested supernatant}}{\text{Minerals in sample}} \times 100 \quad (6)$$

2.9. Statistical Analysis

The data were expressed as the mean value ± standard deviation (SD), all experiments were carried out at least in triplicate. Statistically significant differences were determined using Duncan's multiple range test, performed with SPSS software (version 20.0), at a significance level of $p \leq 0.05$. A one-sample *t*-test was conducted to compare predicted and experimental responses under optimal conditions. Experimental design, regression analysis, and surface plot generation were carried out using Design Expert software (version 8.0.6, Stat-Ease, Inc., Minneapolis, MN, USA) and Minitab 19 (Minitab, LLC, State College, PA, USA). A fitted model based on the experimental data was developed, and the statistical significance of the model terms was assessed through regression analysis and analysis of variance (ANOVA).

3. Results and Discussion

3.1. Effects of Independent Factors on PA and WU-AX

The individual effects of seven variables on the PA and WU-AX contents are shown in Figure 1 and Supplementary Figure S1. These factors can be categorized into two behavioral patterns. The first pattern shows a sharp initial decrease in anti-nutrient levels, followed by stabilization (Figure 1a and Figure S1). Fermentation time and inoculum dose exhibit this behavior. As fermentation time increased and inoculum dose was elevated, the PA and WU-AX contents initially dropped significantly, from 12 to 9 mg/g and 109 to 90 mg/g, respectively, before reaching stable levels of approximately 8.3 mg/g and 88.6 mg/g. The

second pattern, observed in the effects of fermentation temperature, initial pH, substrate particle size, substrate filling rate, and the material-to-liquid ratio, follows a broad "U" shape. Anti-nutrient content changed slowly throughout the process, decreasing at lower levels of the independent variables, remaining relatively stable at medium levels, and increasing gradually at higher levels (Figure 1b and Figure S1). Further analysis suggests that factors such as temperature, time, initial pH, inoculum dose, substrate filling rate, particle size, and the material-to-liquid ratio play key roles in influencing the growth and metabolic activity of *Bacillus subtilis*, thereby affecting the fermentation progression and anti-nutrient degradation.

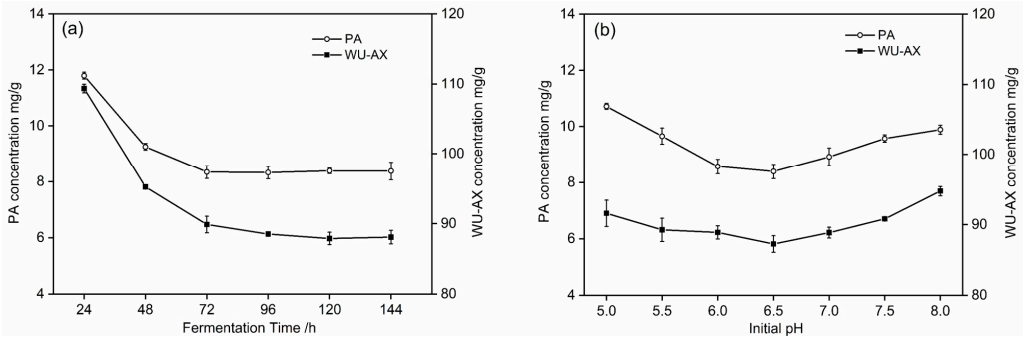

Figure 1. Effects of fermentation time (**a**) and initial pH (**b**) on the PA and WU-AX contents. PA, phytic acid; WU-AX, water-unextractable arabinoxylan.

As shown in Figure 1a, the contents of PA and WU-AX decrease rapidly with increasing fermentation time. However, after 72 h of fermentation, the rate of reduction for both PA and WU-AX slows down significantly. Therefore, considering the perspective of cost saving, 72 h was chosen as the central point for the subsequent optimization process. At the beginning of the fermentation stage, more nutrients were available in the MGF, which could meet the rapid growth needs of the strains. With the extension of the fermentation time, the nutrients in the fermentation material were consumed more, and the strains began to gradually age, and the amount of enzyme production was also reduced gradually. At the same time, as the fermentation proceeds, the substrate surface becomes sticky, the gap between MGF becomes narrow, and the effective diffusion coefficients of both oxygen and carbon dioxide are reduced, which is unfavorable to the enzyme production of *Bacillus subtilis*.

Bacillus subtilis exhibits social cell behavior, with its growth highly dependent on cell density [17]. An appropriate inoculum dose is positively correlated with the growth of *Bacillus subtilis* and production of metabolic components. Too little inoculum is detrimental to the growth of the microorganisms and will increase the microbial latency period, while too much inoculum brings excessive metabolic by-products and accelerates the senescence of the microorganisms [32]. Since the reduction in anti-nutrients was the primary objective of this study, 15% was selected for further study. Although *Bacillus subtilis* possesses heat resistance, high temperatures are not conducive to enzyme production. Additionally, temperature plays a key role in energy consumption during fermentation. A fermentation temperature of 28–34 °C was found to be most effective for reducing PA and WU-AX levels. The pH of the substrate influences both the cell membrane of the microorganism and the intracellular enzymes. Our findings suggest that the optimal pH for the degradation of PA and WU-AX is approximately 6.5. Additionally, pH levels were measured at the final stages of fermentation, showing that under varying fermentation conditions, the final pH was consistently around 8.3, with no significant differences between conditions. Our findings align with previous studies [33], demonstrating that *Bacillus subtilis* fermentation leads to an increase in the pH of the fermentation substrate. Being an aerobic bacterium, *Bacillus subtilis* requires sufficient oxygen for growth [17]. The particle size of the substrate (MGF) affects the growth of *Bacillus subtilis*; larger particles may inhibit nutrient utilization, while smaller particles may hinder oxygen penetration. Therefore, a particle size range of

30–189 μm was selected for further study. Similar analyses were conducted to determine the optimal substrate filling rate and material-to-liquid ratio.

To achieve the greatest reduction in PA and WU-AX, the following factors and levels were selected for further fermentation experiments with *Bacillus subtilis*: fermentation time (48–96 h), temperature (28–34 °C), initial pH (6.0–7.0), inoculum dose (10–20%), particle size (30–189 μm), substrate filling rate (1.84–3.42% in 380 mL glass), and material-to-liquid ratio (1:2.5–1:3.5).

3.2. Screening of Significant Factors Using Plackett–Burman Design

The Plackett–Burman design was employed to assess the significance of independent variables on the contents of PA and WU-AX during the fermentation process and to identify the most critical factors for further optimization. The experimental design and corresponding responses (Y_1, content of PA; and Y_2, content of WU-AX) are presented in Table 1, with the ANOVA results shown in Table 2. Generally, variables with a *p*-value less than 0.05 are considered significant parameters at the 95% confidence interval [19]. The findings revealed that the factors exhibited similar significance for both responses, with X_1 (fermentation time), X_4 (inoculum dose), and X_7 (material-to-liquid ratio) being statistically significant ($p \leq 0.05$). In contrast, X_2 (fermentation temperature), X_3 (initial pH), X_5 (particle size), and X_6 (substrate filling rate) were determined to be non-significant.

As follows, the first-order model equations for PA and WU-AX content were developed using the Plackett–Burman design.

$$Y_1 = 8.8583 - 0.3950X_1 - 0.0567X_2 + 0.0283X_3 - 0.2133X_4 + 0.0350X_5 - 0.0867X_6 - 0.2633X_7 \quad (7)$$

$$Y_2 = 91.8450 - 2.4283X_1 - 0.0733X_2 + 0.2683X_3 - 1.5533X_4 + 0.3383X_5 - 0.3233X_6 - 1.4833X_7 \quad (8)$$

where Y_1 represents the phytic acid (PA) content, Y_2 denotes the water-unextractable arabinoxylan (WU-AX) content, and X_1, X_2, X_3, X_4, X_5, X_6, and X_7 correspond to the coded variables of fermentation time, fermentation temperature, initial pH, inoculum dose, particle size, substrate filling rate, and the material-to-liquid ratio, respectively.

Table 1. Experimental design and response values of Plackett–Burman design.

	Factors							Responses	
Run	**X_1**	**X_2**	**X_3**	**X_4**	**X_5**	**X_6**	**X_7**	**Y_1**	**Y_2**
1	96 (+)	28 (−)	7 (+)	20 (+)	189 (−)	3.42 (+)	1:2.5 (−)	8.6 ± 0.54	88.9 ± 0.94
2	96 (+)	28 (−)	6 (−)	10 (−)	30 (+)	3.42 (+)	1:3.5 (+)	8.3 ± 0.26	90.0 ± 1.88
3	48 (−)	34 (+)	6 (−)	10 (−)	189 (−)	3.42 (+)	1:3.5 (+)	9.1 ± 0.20	92.3 ± 1.01
4	48 (−)	28 (−)	6 (−)	10 (−)	189 (−)	1.84 (−)	1:2.5 (−)	9.9 ± 0.36	97.9 ± 1.40
5	72 (0)	31 (0)	6.5 (0)	15 (0)	123 (0)	2.63 (0)	1:3 (0)	8.3 ± 0.30	87.8 ± 1.24
6	48 (−)	34 (+)	7 (+)	10 (−)	30 (+)	1.84 (−)	1:2.5 (−)	10.0 ± 0.38	98.3 ± 0.84
7	96 (+)	34 (+)	6 (−)	20 (+)	30 (+)	1.84 (−)	1:3.5 (+)	8.2 ± 0.33	86.9 ± 0.96
8	48 (−)	28 (−)	7 (+)	20 (+)	30 (+)	1.84 (−)	1:3.5 (+)	8.7 ± 0.31	91.8 ± 0.91
9	96 (+)	28 (−)	7 (+)	10 (−)	189 (−)	1.84 (−)	1:3.5 (+)	8.4 ± 0.07	89.3 ± 0.57
10	96 (+)	34 (+)	6 (−)	20 (+)	189 (−)	1.84 (−)	1:2.5 (−)	8.5 ± 0.31	88.8 ± 1.08
11	96 (+)	34 (+)	7 (+)	10 (−)	30 (+)	3.42 (+)	1:2.5 (−)	8.8 ± 0.74	92.5 ± 0.59
12	48 (−)	34 (+)	7 (+)	20 (+)	189 (−)	3.42 (+)	1:3.5 (+)	8.9 ± 0.40	91.8 ± 0.43
13	48 (−)	28 (−)	6 (−)	20 (+)	30 (+)	3.42 (+)	1:2.5 (−)	9.0 ± 0.43	93.6 ± 0.92

Note: X_1, fermentation time, hour; X_2, fermentation temperature, °C; X_3, initial pH; X_4, inoculum dose, %; X_5, particle size, μm; X_6, substrate filling rate, %; X_7, material-to-liquid ratio; Y_1, the content of phytic acid (PA), mg/g; Y_2, the content of water-unextractable arabinoxylan (WU-AX), mg/g. Values of Y_1 and Y_2 are given as means ± standard deviation (n = 3).

Table 2. ANOVA of fractional factorial design data for prediction of the PA and WU-AX contents.

PA (Phytic Acid)						
Source	**Sum of Squares**	**Degree of Freedom**	**Mean Square**	**F-Value**	***p*-Value**	**Significance**
Model	3.4036	7	0.4862	10.4564	0.0194	*
X_1	1.8723	1	1.8723	40.2645	0.0032	**
X_2	0.0385	1	0.0385	0.8287	0.4142	
X_3	0.0096	1	0.0096	0.2072	0.6726	
X_4	0.5461	1	0.5461	11.7448	0.0266	*
X_5	0.0147	1	0.0147	0.3161	0.6040	
X_6	0.0901	1	0.0901	1.9384	0.2363	
X_7	0.8321	1	0.8321	17.8953	0.0134	*
WU-AX (Water-Unextractable Arabinoxylan)						
Source	**Sum of Squares**	**Degree of Freedom**	**Mean Square**	**F-Value**	***p*-Value**	**Significance**
Model	129.6758	7	18.5251	17.4466	0.0075	**
X_1	70.7616	1	70.7616	66.6420	0.0012	**
X_2	0.0645	1	0.0645	0.0608	0.8174	
X_3	0.8640	1	0.8640	0.8137	0.4180	
X_4	28.9541	1	28.9541	27.2685	0.0064	**
X_5	1.3736	1	1.3736	1.2937	0.3189	
X_6	1.2545	1	1.2545	1.1815	0.3382	
X_7	26.4033	1	26.4033	24.8662	0.0076	**

Note: X_1, fermentation time, hour; X_2, fermentation temperature, °C; X_3, initial pH; X_4, inoculum dose, %; X_5, particle size, μm; X_6, substrate filling rate, %; X_7, material-to-liquid ratio; statistical significance: * $p < 0.05$, ** $p < 0.01$.

Based on the ANOVA, the factors influencing response Y_1 (PA content) in decreasing order of significance were as follows: X_1 (fermentation time) > X_7 (material-to-liquid ratio) > X_4 (inoculum dose) > X_6 (substrate filling rate) > X_2 (fermentation temperature) > X_5 (particle size) > X_3 (initial pH). For response Y_2 (WU-AX content), the ranking was $X_1 > X_4 > X_7 > X_5 > X_6 > X_3 > X_2$. A Pareto chart can present the effect of factors on responses and check the statistical significance; thus, it was employed here to identify the significant factors [34]. The relative size of the effect degree of each parameter on the PA and WU-AX contents was evaluated by comparing the t-value of the effect. The resulting Pareto chart plotted by the t-value of the effect versus each parameter is shown in Figure 2. A parameter with a t-value higher than the t-value limit line indicated that it had a confidence level greater than 95% and could be considered as significant [35]. In addition, a Bonferroni limit line (5.74) and t-value limit line (2.77) were applied to determine the extremely significant (the t-value was above the Bonferroni limit line), significant (t-value was between the Bonferroni limit line and the t-value limit line), and insignificant (below the t-value limit line) coefficients of different factors [35]. The t-value of the fermentation time, material-to-liquid ratio, and inoculum dose on both responses were above the t-value limit line, which indicated that the three factors were considered as significant factors. Consequently, the fermentation time (X_1), inoculum dose (X_4), and material-to-liquid ratio (X_7) were selected for the further optimization of fermentation conditions. Both fermentation time and inoculum dose have been identified as critical parameters in other fermentation processes as well. In light of the Plackett–Burman design results, and considering fermentation efficiency and cost considerations, the non-significant variables—fermentation temperature, initial pH, particle size, and substrate filling rate—were fixed at 31 °C, pH 6.5, 189 μm, and 2.63%, respectively.

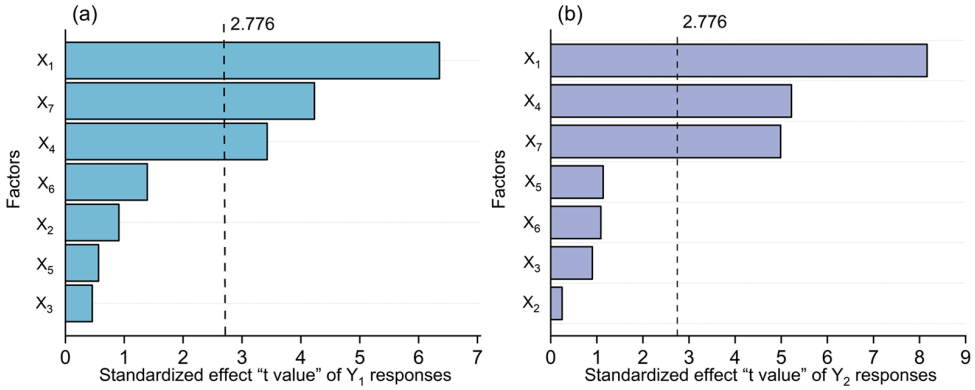

Figure 2. Pareto chart illustrating the effects of seven variables on the responses of Y_1 (**a**) and Y_2 (**b**). Variables with t-values exceeding the critical value of 2.77 are considered statistically significant. X_1, fermentation time, hour; X_2, fermentation temperature, °C; X_3, initial pH; X_4, inoculum dose, %; X_5, particle size, μm; X_6, substrate filling rate, %; X_7, material-to-liquid ratio; Y_1, the content of phytic acid (PA), mg/g; Y_2, the content of water-unextractable arabinoxylan (WU-AX), mg/g.

3.3. Statistical Analysis of Central Composite Design

The factors and levels of variables in the response-surface central composite design arrangement and experimental responses of PA content (Y_1) and WU-AX content (Y_2) are presented in Table 3. Multiple regression analysis was carried out on the experimental data, and the second-order polynomial stepwise equations were obtained, as shown in Equations (9) and (10).

$$Y_1 = 8.41 - 0.40X_1 - 0.24X_4 - 0.25X_7 + 0.19X_1X_4 - 0.001X_1X_7 - 0.042X_4X_7 + 0.27X_1^2 + 0.30X_4^2 + 0.17X_7^2 \quad (9)$$

$$Y_2 = 85.56 - 3.65X_1 - 2.80X_4 - 1.57X_7 - 0.20X_1X_4 + 1.76X_1X_7 - 0.53X_4X_7 + 3.11X_1^2 + 2.38X_4^2 + 0.92X_7^2 \quad (10)$$

where Y_1 represents the phytic acid (PA) content, Y_2 denotes the water-unextractable arabinoxylan (WU-AX) content, and X_1, X_4, and X_7 are the coding variables of fermentation time, inoculum dose, and the material-to-liquid ratio, respectively.

Table 3. Central composite design with experimental responses for the PA and WU-AX contents in MGF under different fermentation conditions.

	Factors			Responses	
Run	**X_1**	**X_4**	**X_7**	**Y_1**	**Y_2**
5	48 (−1)	10 (−1)	1:3.5 (1)	9.7 ± 0.27	94.8 ± 0.70
1	48 (−1)	10 (−1)	1:2.5 (−1)	10.2 ± 0.46	102.2 ± 1.59
12	72 (0)	25 (2)	1:3 (0)	8.9 ± 0.32	89.5 ± 1.25
13	72 (0)	15 (0)	1:2 (−2)	9.4 ± 0.13	90.9 ± 1.13
4	96 (1)	20 (1)	1:2.5 (−1)	9.3 ± 0.17	87.1 ± 0.32
16 (C)	72 (0)	15 (0)	1:3 (0)	8.3 ± 0.30	83.5 ± 1.46
10	120 (2)	15 (0)	1:3 (0)	8.4 ± 0.30	89.7 ± 0.80
8	96 (1)	20 (1)	1:3.5 (1)	8.6 ± 0.25	84.6 ± 0.65
3	48 (−1)	20 (1)	1:2.5 (−1)	9.2 ± 0.70	97.0 ± 0.73
2	96 (1)	10 (−1)	1:2.5 (−1)	9.2 ± 0.07	91.7 ± 0.97
7	48 (−1)	20 (1)	1:3.5 (1)	9.0 ± 0.36	88.9 ± 0.99
6	96 (1)	10 (−1)	1:3.5 (1)	8.7 ± 0.31	92.8 ± 1.05
19 (C)	72 (0)	15 (0)	1:3 (0)	8.3 ± 0.29	87.9 ± 0.56
17 (C)	72 (0)	15 (0)	1:3 (0)	8.2 ± 0.46	84.5 ± 0.72
14	72 (0)	15 (0)	1:4 (2)	8.6 ± 0.25	86.8 ± 0.91
9	24 (−2)	15 (0)	1:3 (0)	10.4 ± 0.44	105.5 ± 0.78
11	72 (0)	5 (−2)	1:3 (0)	10.1 ± 0.19	99.9 ± 1.08
18 (C)	72 (0)	15 (0)	1:3 (0)	8.4 ± 0.28	85.8 ± 1.24
15 (C)	72 (0)	15 (0)	1:3 (0)	8.6 ± 0.61	85.3 ± 0.51

Note: X_1, fermentation time, h; X_4, inoculum dose, %; X_7, material-to-liquid ratio; Y_1, phytic acid (PA) content, mg/g; Y_2, water-unextractable arabinoxylan (WU-AX) content, mg/g. Values of Y_1 and Y_2 are given as means ± standard deviation (n = 3).

These equations demonstrate the quantitative impact of the factors (X_1, X_4, and X_7) and their interactions on the response variables. ANOVA was performed to assess the significance of the central composite design model and validate the accuracy of the fitting curve [36]. The model coefficients were evaluated using F-values and *p*-values, with a higher F-value and smaller *p*-value ($p \leq 0.05$) indicating greater model significance [19,34,36]. The ANOVA results, along with goodness-of-fit and model adequacy, are presented in Table 4. The model coefficients were validated based on F-values and *p*-values. As shown, the F-values and corresponding low *p*-values for both the PA and WU-AX responses confirmed the high significance of the models. The lack of fit for both response models was insignificant ($p > 0.05$), with values of 0.2272 and 0.6234 for PA and WU-AX, respectively. This suggests that no outliers were present in the data, and higher-order terms were unnecessary, confirming the appropriateness of the selected models. The high coefficient of determination (R^2), 0.9469 for PA and 0.9712 for WU-AX, indicates that the factor terms explain 94.69% and 97.12% of the variance in the models for PA and WU-AX, respectively, implying the models are reliable. Furthermore, the R^2 values were close to their respective adjusted R^2 values, further demonstrating the high explanatory power of the regression models used in this study [19]. The coefficient of variation (CV) values, which reflect the degree of variability in the mean response, were 2.45% for PA and 1.67% for WU-AX, indicating low variability between the predicted and experimental responses. Therefore, the mathematical models established in this study have been proven reliable and can be utilized for subsequent prediction and optimization steps.

Table 4. ANOVA of central composite design for the PA and WU-AX contents in MGF under different fermentation conditions.

Source	PA			WU-AX		
	Sum of Squares	**F-Value**	***p*-Value**	**Sum of Squares**	**F-Value**	***p*-Value**
Model	7.8627	17.8433	0.0001	696.2109	33.6951	<0.0001
X_1	2.5440	51.9596	<0.0001	213.1600	92.4500	<0.0001
X_4	0.9312	19.0195	0.0018	125.3280	54.3563	<0.0001
X_7	0.9702	19.8160	0.0016	39.4384	17.1049	0.0025
$X_1 \times X_4$	0.2813	5.7443	0.0401	0.3200	0.1388	0.7181
$X_1 \times X_7$	0.0008	0.0163	0.9011	24.7808	10.7477	0.0096
$X_4 \times X_7$	0.0145	0.2951	0.6001	2.2261	0.9655	0.3515
X_1^2	1.7536	35.8157	0.0002	229.7474	99.6442	<0.0001
X_4^2	2.0730	42.3401	0.0001	134.6781	58.4115	<0.0001
X_7^2	0.7016	14.3295	0.0043	20.0899	8.7132	0.0162
Residual	0.4407			20.7511		
Lack of Fit	0.3247	2.2411	0.2272	10.0901	0.7572	0.6234
C.V.%	2.45			1.67		
Pure Error	0.1159			10.6610		
Cor Total	8.3034			719.9620		
R^2	0.9469			0.9712		
R^2-adjusted	0.8939			0.9424		

Note: X_1, X_4, and X_7 represent the linear effects of fermentation time (h), inoculum dose (%), and the material-to-liquid ratio, respectively. X_1^2, X_4^2, and X_7^2 denote the quadratic effects, while $X_1 \times X_4$, $X_1 \times X_7$, and $X_4 \times X_7$ represent the interaction effects.

The response-surface three-dimensional graphs were generated based on the second-order polynomial equation to analyze the interaction and quadratic effects of the variables. The changes in model parameters were examined by varying two factors while holding the remaining factors constant at their central levels. The three-dimensional representations of the interaction and quadratic effects on PA and WU-AX contents are shown in Figures 3 and 4, respectively. These response-surface plots all tended to flatten out towards the fermentation time side, and the PA and WU-AX contents decreased significantly and

stabilized at the later stages of fermentation, which was consistent with the results of the one-way experiments (Figure 1a). The coefficients of the linear terms (X_1, X_4, and X_7) and the quadratic terms (X_1^2, X_4^2, and X_7^2) were statistically significant for both PA and WU-AX responses ($p \leq 0.05$). The two-factor interaction term X_1X_4 had a significant effect ($p \leq 0.05$) on PA, while the interaction term X_1X_7 showed a significant influence ($p \leq 0.05$) on WU-AX. Notably, X_1 had the most significant effect, followed by X_7 and X_4 for the PA response. In contrast, for the WU-AX response, the order of variable influence was $X_1 > X_4 > X_7$ (Table 4). These significant effects of X_1, X_4, and X_7 are consistent with the results of the significance analysis in the Plackett–Burman design. The values of the interaction terms further indicated strong interactions between the independent variables, particularly X_1X_4 for the PA response and X_1X_7 for the WU-AX response.

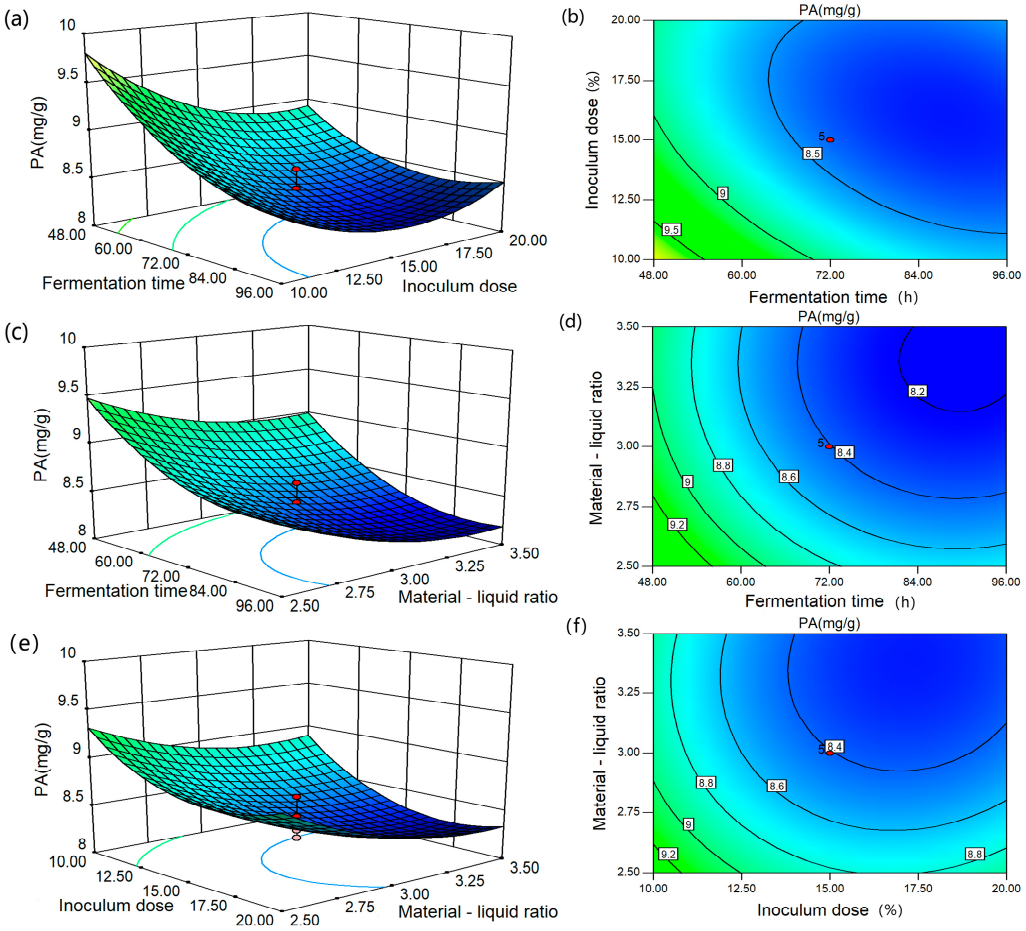

Figure 3. Response-surface plots illustrating the effects on PA content and the interactions between (**a**) fermentation time and inoculum dose, (**c**) fermentation time and the material-to-liquid ratio, and (**e**) inoculum dose and the material-to-liquid ratio. Corresponding 2D contour plots depict the interactions between (**b**) fermentation time and inoculum dose, (**d**) fermentation time and the material-to-liquid ratio, and (**f**) inoculum dose and the material-to-liquid ratio.

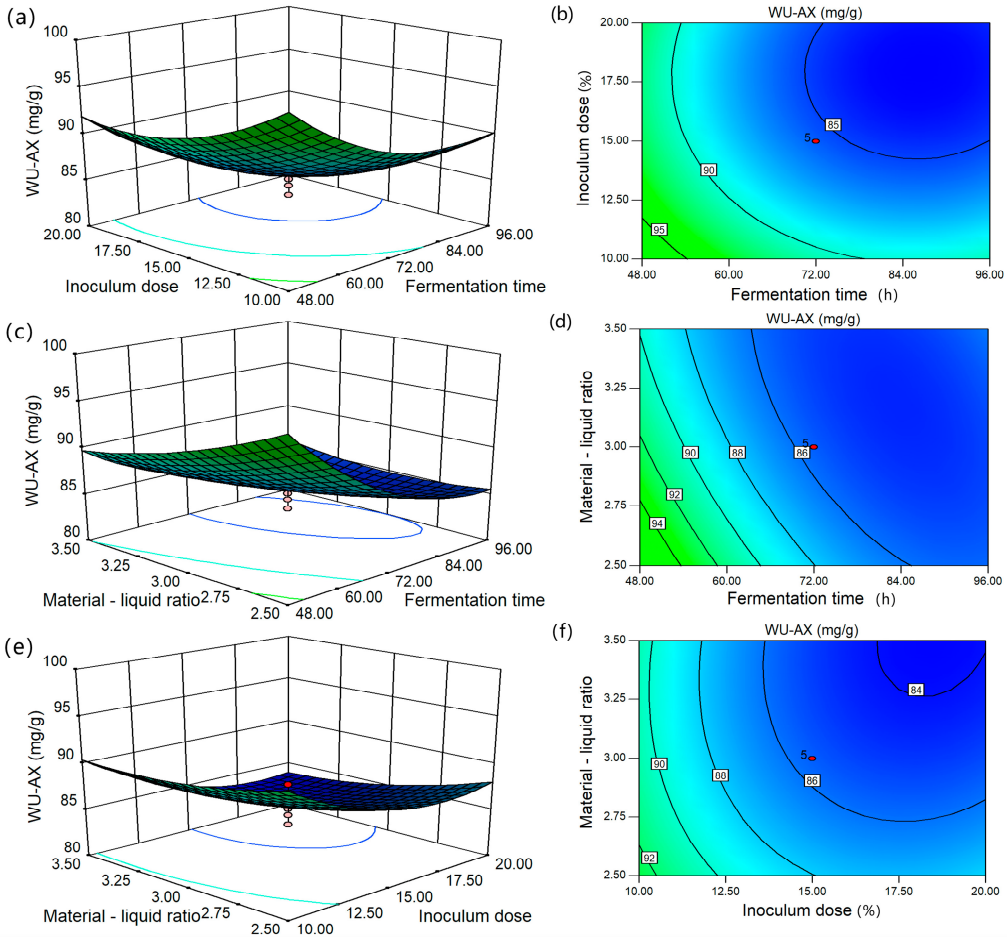

Figure 4. Response-surface plots illustrating the effects on WU-AX content and the interactions between (**a**) fermentation time and inoculum dose, (**c**) fermentation time and the material-to-liquid ratio, and (**e**) inoculum dose and the material-to-liquid ratio. Corresponding 2D contour plots depict the interactions between (**b**) fermentation time and inoculum dose, (**d**) fermentation time and the material-to-liquid ratio, and (**f**) inoculum dose and the material-to-liquid ratio.

3.4. Optimum Conditions and Authenticity of Predictive Model

Further analysis of the model optimization revealed that the theoretical optimal fermentation parameters for MGF were 84.48 h, a 17.09% inoculum dose, and a material-to-liquid ratio of 1:3.35. To enhance operational feasibility, the optimal fermentation conditions were adjusted as follows: raw materials were ground to pass through an 80-mesh sieve, with a material-to-liquid ratio of 1:3.4, an initial pH of 6.5, and a fermentation vessel filling rate of 2.6%. An inoculum dose of 17.1% was used, with fermentation conducted for 84.5 h at 31 °C. Under these optimal conditions, the predicted PA and WU-AX contents were 8.16 mg/g and 83.55 mg/g, respectively. To verify the accuracy of the model, triplicate validation experiments were performed under the optimal conditions, and the experimental results were compared to the predicted values. The observed PA and WU-AX contents were 8.2 ± 0.78 mg/g and 83.1 ± 1.09 mg/g, respectively, which were in close agreement with the predicted values. This strong correlation confirmed the model's adequacy in predicting the optimization outcomes. When comparing the PA and WU-AX contents of untreated MGF samples, which were 16.0 mg/g and 122.1 mg/g, respectively, fermentation under the optimized conditions reduced their levels by 48% and 32%, respectively.

3.5. Changes in Enzymatic Activity Before and After Fermentation

The product obtained from MGF through the optimized fermentation process is referred to as FMGF (fermented maize gluten feed, FMGF). The enzymatic activities of

phytase, xylanase, cellulase, and protease were compared between MGF and FMGF. As shown in Figure 5, the activities of all four enzymes—phytase, xylanase, cellulase, and protease—significantly increased after fermentation with *Bacillus subtilis* ($p < 0.001$). Under optimal fermentation conditions, FMGF exhibited a phytase activity of 8.2 ± 0.24 U/g, xylanase activity of 126.3 ± 6.24 U/g, cellulase activity of 19.3 ± 0.87 U/g, and protease activity of 1182 ± 87 U/g, respectively.

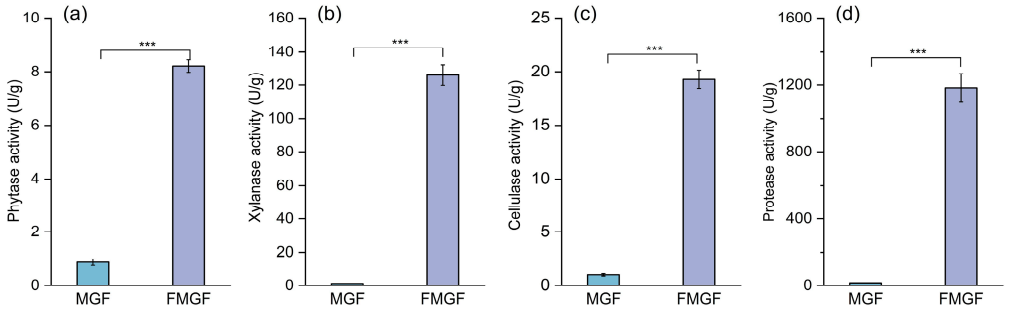

Figure 5. Effects of fermentation on the activities of phytase (**a**), xylanase (**b**), cellulase (**c**), and protease (**d**). MGF, maize germ feed; FMGF, fermented maize germ feed; *** means significance level of $p < 0.001$.

PA, also known as myo-inositol hexaphosphate, is considered an anti-nutrient because it can form complexes with minerals, starch, and proteins, thereby limiting their bioavailability [37]. Phytase, secreted by *Bacillus subtilis* during fermentation, degrades myo-inositol hexaphosphate into inositol and free phosphates. AX predominantly exists in the form of WU-AX, which diminishes nutrient absorption through sequestration within cell walls via covalent or non-covalent interactions [10,12]. Xylanase, a complex enzyme system capable of hydrolyzing both the main and side chains of xylan, breaks down WU-AX into smaller fragments, disrupting the fiber structure and releasing nutrients [38,39]. Some researchers have suggested that xylanase and phytase work synergistically, with xylanase degrading non-starch polysaccharides to facilitate phytase-mediated PA degradation, thereby releasing additional nutrients [38]. Cellulase, a multi-component enzyme composed of endoglucanase, cellobiohydrolase, and β-glucosidase, is responsible for converting cellulose into soluble saccharides, providing energy for *Bacillus subtilis* growth [40]. Neutral protease, an extracellular protease produced by *Bacillus subtilis*, has an optimal pH range between 6.0 and 7.5 and hydrolyzes proteins into small peptides and amino acids. These proteases are produced after the exponential growth phase and are believed to play a role in spore formation, cell wall turnover, and enzyme clearance [28]. A previous study has demonstrated that *Bacillus subtilis* possesses the capacity to secrete a diverse array of enzymes during fermentation processing, including protease, phytase, and cellulase [17]. The combined action of cellulase, xylanase, phytase, and protease disrupts the surface integrity of MGF cell walls, leading to the disruption of the fibrous network structure of cellulose, thereby facilitating the release of bound nutritional components. Furthermore, the combination of microbial fermentation with enzyme activity results in a multi-enzyme approach, producing not only phytase but also xylanase, cellulase, and protease, which together act synergistically to break down the complex structures of anti-nutritional factors. This multi-faceted enzymatic action makes fermentation with *Bacillus subtilis* a more holistic and effective treatment method compared to the single-enzyme supplementation strategies commonly used in the industry.

3.6. Comparison of the Nutritional Values of MGF and FMGF

As shown in Table 5, the fermentation of MGF resulted in an increase in crude protein from 27.1 ± 0.13% to 28.6 ± 0.08%, PDI from 37.9 ± 1.02% to 46.7 ± 0.58%, DH from 2.3 ± 0.11% to 3.3 ± 0.12%, and IVPD from 44.3 ± 1.07% to 58.5 ± 0.78%, respectively. The increase in protein was primarily attributed to a relative loss of dry matter due to microbial

hydrolysis and the metabolism of carbohydrates and lipids as an energy source [28]. Our results demonstrated that *Bacillus subtilis* produced proteases, which hydrolyzed proteins into soluble peptides or amino acids, resulting in significant increases in PDI, DH, and IVPD ($p < 0.001$). PDI reflects the proportion of protein dispersed in water under controlled extraction conditions and serves as an indicator of protein solubility. Fermentation significantly improved the water solubility of MGF proteins. DH represents the percentage of free amino nitrogen relative to the total nitrogen content; the proteolytic activity during fermentation exposed more amino groups, resulting in an increased DH. The DH calculation method used in this study follows Zhang et al. [28], differing from many other methods in the literature [41], as it does not subtract the original free amino nitrogen in MGF, allowing for a more accurate comparison between FMGF and raw MGF.

Table 5. Protein nutritional analysis results and in vitro minerals digestion of MGF and FMGF.

Items	MGF	FMGF	*p*-Value	Change (%)
Protein (%)	27.1 ± 0.13	28.63 ± 0.08	<0.001	5.57
PDI (%)	37.9 ± 1.02	46.67 ± 0.58	<0.001	23.17
DH (%)	2.3 ± 0.11	3.26 ± 0.12	<0.001	43.61
IVPD (%)	44.3 ± 1.07	58.48 ± 0.78	<0.001	31.92
Minerals' bioavailability				
Fe (%)	22.8 ± 1.51	33.68 ± 2.15	<0.001	47.72
Mn (%)	38.3 ± 1.53	53.23 ± 1.38	<0.001	39.05
Cu (%)	46.0 ± 1.04	57.54 ± 1.06	<0.001	25.20
Zn (%)	12.6 ± 1.23	16.67 ± 0.95	<0.001	31.88

Note: Cu, copper; DH, degree of hydrolysis; Fe, iron; FMGF, fermented maize gluten feed; IVPD, in vitro protein digestion; MGF, maize gluten feed; Mn, manganese; PDI, protein dispersibility index; Zn, zinc.

Compared to MGF, FMGF exhibited a significant 31.92% increase in IVPD. The IVPD assessment method employed in this study is a classical two-step pepsin–trypsin digestion model, which closely correlates with the in vivo protein digestibility results obtained from rat feeding trials [42]. The increased of IVPD of FMGF can be attributed to three primary factors: the proteases produced during fermentation partially break down proteins into smaller peptides or amino acids; the structural alterations in proteins following fermentation increase their susceptibility to protease activity, making them easier to hydrolyze; and the degradation of anti-nutritional factors like PA and WU-AX further enhances protein digestibility.

Additionally, the bioavailability of essential minerals (Fe, Mn, Cu, and Zn) in MGF increased following fermentation, with Fe increasing from 22.8 ± 1.51% to 33.7 ± 2.15%, Mn from 38.3 ± 1.5% to 53.2 ± 1.38%, Cu from 46.0 ± 1.04% to 57.5 ± 1.06%, and Zn from 12.6 ± 1.23% to 16.7 ± 0.95%. These findings suggest that fermentation with *Bacillus subtilis* significantly enhances the bioavailability of essential minerals in MGF, thereby improving its overall nutritional value. PA forms covalent bonds with minerals, rendering them resistant to digestion in the mammalian gastrointestinal system and impairing mineral absorption. Additionally, WU-AX binds minerals through both covalent and non-covalent interactions. Our results indicate that *Bacillus subtilis* fermentation effectively degrades PA and WU-AX in MGF, releasing bound minerals and thus increasing their bioavailability.

4. Conclusions

Fermentation with *Bacillus subtilis* presents a promising technology for the degradation of anti-nutrients, phytic acid, and water-unextractable arabinoxylans, in maize gluten feed. Among the seven parameters studied, the fermentation time, inoculum dose, and material-to-liquid ratio were identified as the most influential factors. Notably, the interactions between fermentation time and inoculum dose, as well as between fermentation time and the material-to-liquid ratio, significantly impacted the degradation of anti-nutritional factors. The optimal fermentation conditions were determined as follows: raw materials ground to pass through an 80-mesh sieve, a material-to-liquid ratio of 1:3.4, an initial pH of 6.5, and a fermentation vessel filling rate of 2.6%. An inoculum dose of 17.1%

was applied, followed by fermentation for 84.5 h at 31 °C. Under these conditions, the post-fermentation contents of phytic acid and water-unextractable arabinoxylans were 8.2 ± 0.78 mg/g and 83.2 ± 1.09 mg/g, respectively—representing reductions of 48% and 32% compared to the raw materials. The fermented maize gluten feed exhibited enhanced protease, xylanase, phytase, and cellulase activity, which facilitated the breakdown of phytic acid and water-unextractable arabinoxylans. Additionally, fermented maize gluten feed showed significant increases in the protein dispersibility index, in vitro protein digestibility, and mineral bioavailability compared with unfermented maize gluten feed. While the current experimental results are promising, they have been obtained on a laboratory scale, and further validation is necessary for industrial applications. We have also identified potential avenues for future research, including investigating the effects of fermentation on the functional and structural properties of maize gluten feed (MGF), comparing the efficacy of fermentation treatment with that of commercial enzyme treatments, and assessing the impact on animal growth performance. In conclusion, this fermentation process offers an efficient method for reducing anti-nutritional factors in maize gluten feed, with substantial potential for producing nutritionally improved food ingredients.

Supplementary Materials: The following supporting information can be downloaded at https://www.mdpi.com/article/10.3390/fermentation10110555/s1, Figure S1: Effects of fermentation conditions on PA and WU-AX contents. The univariate tests were of the fermentation temperature (a), inoculum dose (b), particle size (c), substrate filling rate (d), and material-to-liquid ratio (e). PA, phytic acid; WU-AX, water-unextractable arabinoxylans; Table S1: Factors and levels of Plackett–Burman experimental design.

Author Contributions: Conceptualization, X.S. and J.L.; methodology, X.S.; software, L.M.; validation, Y.X. and L.M.; writing—original draft preparation, X.S.; writing—review and editing, X.S.; supervision, J.L.; project administration, J.L.; funding acquisition, J.L. and X.S. All authors have read and agreed to the published version of the manuscript.

Funding: This project was funded by the Deutsche Forschungsgemeinschaft (DFG, German Research Foundation; 328017493/GRK 2366; International Research Training Group "Adaption of maize-based food-feed-energy systems to limited phosphate resources"). This work was also supported by the Special Fund for Introduced Talent to Initiate Scientific Research of Zhejiang Ocean University, China (JX6311130923).

Institutional Review Board Statement: Not applicable.

Informed Consent Statement: Not applicable.

Data Availability Statement: Data are contained within the article.

Conflicts of Interest: The authors declare no conflicts of interest.

References

1. Zhang, R.; Ma, S.; Li, L.; Zhang, M.; Tian, S.; Wang, D.; Liu, K.; Liu, H.; Zhu, W.; Wang, X. Comprehensive Utilization of Corn Starch Processing By-Products: A Review. *Grain Oil Sci. Technol.* **2021**, *4*, 89–107. [CrossRef]
2. Guo, Y.; Wang, K.; Wu, B.; Wu, P.; Duan, Y.; Ma, H. Production of ACE Inhibitory Peptides from Corn Germ Meal by an Enzymatic Membrane Reactor with a Novel Gradient Diafiltration Feeding Working-Mode and in vivo Evaluation of Antihypertensive Effect. *J. Funct. Foods* **2020**, *64*, 103584. [CrossRef]
3. Rocha-Villarreal, V.; Hoffmann, J.F.; Vanier, N.L.; Serna-Saldivar, S.O.; García-Lara, S. Hydrothermal Treatment of Maize: Changes in Physical, Chemical, and Functional Properties. *Food Chem.* **2018**, *263*, 225–231. [CrossRef] [PubMed]
4. Lyu, Z.; Li, Y.; Liu, H.; Li, E.; Li, P.; Zhang, S.; Wang, F.; Lai, C. Net Energy Content of Rice Bran, Defatted Rice Bran, Corn Gluten Feed, and Corn Germ Meal Fed to Growing Pigs Using Indirect Calorimetry. *J. Anim. Sci.* **2018**, *96*, 1877–1888. [CrossRef] [PubMed]
5. Ortiz de Erive, M.; Wang, T.; He, F.; Chen, G. Development of High-Fiber Wheat Bread Using Microfluidized Corn Bran. *Food Chem.* **2020**, *310*, 125921. [CrossRef]
6. Bloot, A.P.M.; Kalschne, D.L.; Amaral, J.A.S.; Baraldi, I.J.; Canan, C. A Review of Phytic Acid Sources, Obtention, and Applications. *Food Rev. Int.* **2023**, *39*, 73–92. [CrossRef]

7. Shi, C.; Zhang, Y.; Lu, Z.; Wang, Y. Solid-State Fermentation of Corn-Soybean Meal Mixed Feed with *Bacillus subtilis* and *Enterococcus faecium* for Degrading Antinutritional Factors and Enhancing Nutritional Value. *J. Anim. Sci. Biotechnol.* **2017**, *8*, 50. [CrossRef]
8. Sun, X.; Ma, L.; Lux, P.E.; Wang, X.; Stuetz, W.; Frank, J.; Liang, J. The Distribution of Phosphorus, Carotenoids and Tocochromanols in Grains of Four Chinese Maize (*Zea mays* L.) Varieties. *Food Chem.* **2022**, *367*, 130725. [CrossRef]
9. Noureddini, H.; Malik, M.; Byun, J.; Ankeny, A.J. Distribution of Phosphorus Compounds in Corn Processing. *Bioresour. Technol.* **2009**, *100*, 731–736. [CrossRef]
10. Sun, H.; Cozannet, P.; Ma, R.; Zhang, L.; Huang, Y.K.; Preynat, A.; Sun, L.-h. Effect of Concentration of Arabinoxylans and a Carbohydrase Mixture on Energy, Amino Acids and Nutrients Total Tract and Ileal Digestibility in Wheat and Wheat by-Product-Based Diet for Pigs. *Anim. Feed Sci. Technol.* **2020**, *262*, 114380. [CrossRef]
11. Huang, M.; Bai, J.; Buccato, D.G.; Zhang, J.; He, Y.; Zhu, Y.; Yang, Z.; Xiao, X.; Daglia, M. Cereal-Derived Water-Unextractable Arabinoxylans: Structure Feature, Effects on Baking Products and Human Health. *Foods* **2024**, *13*, 2369. [CrossRef] [PubMed]
12. Wang, J.; Bai, J.; Fan, M.; Li, T.; Li, Y.; Qian, H.; Wang, L.; Zhang, H.; Qi, X.; Rao, Z. Cereal-Derived Arabinoxylans: Structural Features and Structure–Activity Correlations. *Trends Food Sci. Technol.* **2020**, *96*, 157–165. [CrossRef]
13. Rosicka-Kaczmarek, J.; Komisarczyk, A.; Nebesny, E.; Makowski, B. The Influence of Arabinoxylans on the Quality of Grain Industry Products. *Eur. Food Res. Technol.* **2016**, *242*, 295–303. [CrossRef]
14. Bautil, A.; Verspreet, J.; Buyse, J.; Goos, P.; Bedford, M.R.; Courtin, C.M. Age-Related Arabinoxylan Hydrolysis and Fermentation in the Gastrointestinal Tract of Broilers Fed Wheat-Based Diets. *Poult. Sci.* **2019**, *98*, 4606–4621. [CrossRef] [PubMed]
15. Endalew, H.W.; Atlabachew, M.; Karavoltsos, S.; Sakellari, A.; Aslam, M.F.; Allen, L.; Griffiths, H.; Zoumpoulakis, P.; Kanellou, A.; Yehuala, T.F.; et al. Effect of Fermentation on Nutrient Composition, Antinutrients, and Mineral Bioaccessibility of Finger Millet Based *Injera*: A Traditional Ethiopian Food. *Food Res. Int.* **2024**, *190*, 114635. [CrossRef] [PubMed]
16. Watanakij, N.; Visessanguan, W.; Petchkongkaew, A. Aflatoxin B_1-Degrading Activity from *Bacillus subtilis* BCC 42005 Isolated from Fermented Cereal Products. *Food Addit. Contam. Part A* **2020**, *37*, 1579–1589. [CrossRef]
17. Iqbal, S.; Begum, F.; Rabaan, A.A.; Aljeldah, M.; Al Shammari, B.R.; Alawfi, A.; Alshengeti, A.; Sulaiman, T.; Khan, A. Classification and Multifaceted Potential of Secondary Metabolites Produced by *Bacillus subtilis* Group: A Comprehensive Review. *Molecules* **2023**, *28*, 927. [CrossRef]
18. Suprayogi, W.P.S.; Ratriyanto, A.; Akhirini, N.; Hadi, R.F.; Setyono, W.; Irawan, A. Changes in Nutritional and Antinutritional Aspects of Soybean Meals by Mechanical and Solid-State Fermentation Treatments with *Bacillus subtilis* and *Aspergillus oryzae*. *Bioresour. Technol. Rep.* **2022**, *17*, 100925. [CrossRef]
19. Bruno Siewe, F.; Kudre, T.G.; Narayan, B. Optimisation of Ultrasound-Assisted Enzymatic Extraction Conditions of Umami Compounds from Fish by-Products Using the Combination of Fractional Factorial Design and Central Composite Design. *Food Chem.* **2021**, *334*, 127498. [CrossRef]
20. Buddrick, O.; Jones, O.A.H.; Cornell, H.J.; Small, D.M. The Influence of Fermentation Processes and Cereal Grains in Wholegrain Bread on Reducing Phytate Content. *J. Cereal Sci.* **2014**, *59*, 3–8. [CrossRef]
21. Douglas, S.G. A Rapid Method for the Determination of Pentosans in Wheat Flour. *Food Chem.* **1981**, *7*, 139–145. [CrossRef]
22. Rouau, X.; Surget, A. A Rapid Semi-Automated Method for the Determination of Total and Water-Extractable Pentosans in Wheat Flours. *Carbohydr. Polym.* **1994**, *24*, 123–132. [CrossRef]
23. Hernández-Espinosa, N.; Posadas-Romano, G.; Dreisigacker, S.; Crossa, J.; Crespo, L.; Ibba, M.I. Efficient Arabinoxylan Assay for Wheat: Exploring Variability and Molecular Marker Associations in Wholemeal and Refined Flour. *J. Cereal Sci.* **2024**, *117*, 103897. [CrossRef] [PubMed]
24. Akpoilih, B.U.; Adeshina, I.; Chukwudi, C.F.; Abdel-Tawwab, M. Evaluating the Inclusion of Phytase Sources to Phosphorus-Free Diets for GIFT Tilapia (*Oreochromis niloticus*): Growth Performance, Intestinal Morphometry, Immune-Antioxidant Responses, and Phosphorus Utilization. *Anim. Feed Sci. Technol.* **2023**, *303*, 115678. [CrossRef]
25. Dhaver, P.; Pletschke, B.; Sithole, B.; Govinden, R. Optimization, Purification, and Characterization of Xylanase Production by a Newly Isolated Trichoderma Harzianum Strain by a Two-Step Statistical Experimental Design Strategy. *Sci. Rep.* **2022**, *12*, 17791. [CrossRef]
26. Al Talebi, Z.A.; Al-Kawaz, H.S.; Mahdi, R.K.; Al-Hassnawi, A.T.; Alta'ee, A.H.; Hadwan, A.M.; Khudhair, D.A.; Hadwan, M.H. An Optimized Protocol for Estimating Cellulase Activity in Biological Samples. *Anal. Biochem.* **2022**, *655*, 114860. [CrossRef]
27. Wang, Y.; Xu, K.; Lu, F.; Wang, Y.; Ouyang, N.; Ma, H. Application of Ultrasound Technology in the Field of Solid-State Fermentation: Increasing Peptide Yield through Ultrasound-Treated Bacterial Strain. *J. Sci. Food Agric.* **2021**, *101*, 5348–5358. [CrossRef]
28. Zhang, Y.; Ishikawa, M.; Koshio, S.; Yokoyama, S.; Dossou, S.; Wang, W.; Zhang, X.; Shadrack, R.S.; Mzengereza, K.; Zhu, K.; et al. Optimization of Soybean Meal Fermentation for Aqua-Feed with *Bacillus Subtilis* Natto Using the Response Surface Methodology. *Fermentation* **2021**, *7*, 306. [CrossRef]
29. Pearce, K.N.; Karahalios, D.; Friedman, M. Ninhydrin Assay For Proteolysis in Ripening Cheese. *J. Food Sci.* **1988**, *53*, 432–435. [CrossRef]
30. Kamble, D.B.; Singh, R.; Rani, S.; Kaur, B.P.; Upadhyay, A.; Kumar, N. Optimization and Characterization of Antioxidant Potential, in vitro Protein Digestion and Structural Attributes of Microwave Processed Multigrain Pasta. *J. Food Process. Preserv.* **2019**, *43*, e14125. [CrossRef]

31. Kumar, A.; Lal, M.K.; Kar, S.S.; Nayak, L.; Ngangkham, U.; Samantaray, S.; Sharma, S.G. Bioavailability of Iron and Zinc as Affected by Phytic Acid Content in Rice Grain. *J. Food Biochem.* **2017**, *41*, e12413. [CrossRef]
32. Zhang, L.; Yang, Y.; Sun, J.; Shen, Y.; Wei, D.; Zhu, J.; Chu, J. Microbial Production of 2,3-Butanediol by a Mutagenized Strain of Serratia Marcescens H30. *Bioresour. Technol.* **2010**, *101*, 1961–1967. [CrossRef] [PubMed]
33. Terlabie, N.N.; Sakyi-Dawson, E.; Amoa-Awua, W.K. The Comparative Ability of Four Isolates of *Bacillus subtilis* to Ferment Soybeans into Dawadawa. *Int. J. Food Microbiol.* **2006**, *106*, 145–152. [CrossRef] [PubMed]
34. Dayana Priyadharshini, S.; Bakthavatsalam, A.K. Optimization of Phenol Degradation by the Microalga *Chlorella Pyrenoidosa* Using Plackett-Burman Design and Response Surface Methodology. *Bioresour. Technol.* **2016**, *207*, 150–156. [CrossRef]
35. Chen, F.; Zhang, Q.; Fei, S.; Gu, H.; Yang, L. Optimization of Ultrasonic Circulating Extraction of Samara Oil from Acer Saccharum Using Combination of Plackett–Burman Design and Box–Behnken Design. *Ultrason. Sonochem.* **2017**, *35*, 161–175. [CrossRef]
36. Xi, J.; Xiang, B.; Deng, Y. Comparison of Batch and Circulating Processes for Polyphenols Extraction from Pomelo Peels by Liquid-Phase Pulsed Discharge. *Food Chem.* **2021**, *340*, 127918. [CrossRef]
37. Chen, W.; Xu, D. Phytic Acid and Its Interactions in Food Components, Health Benefits, and Applications: A Comprehensive Review. *Trends Food Sci. Technol.* **2023**, *141*, 104201. [CrossRef]
38. Dahiya, S.; Kumar, A.; Singh, B. Enhanced Endoxylanase Production by *Myceliophthora thermophila* Using Rice Straw and Its Synergism with Phytase in Improving Nutrition. *Process Biochem.* **2020**, *94*, 235–242. [CrossRef]
39. Tse, T.; Schendel, R.R. Cereal Grain Arabinoxylans: Processing Effects and Structural Changes during Food and Beverage Fermentations. *Fermentation* **2023**, *9*, 914. [CrossRef]
40. Liu, Y.; Li, H.; Liu, W.; Ren, K.; Li, X.; Zhang, Z.; Huang, R.; Han, S.; Hou, J.; Pan, C. Bioturbation Analysis of Microbial Communities and Flavor Metabolism in a High-Yielding Cellulase *Bacillus subtilis* Biofortified Daqu. *Food Chem X* **2024**, *22*, 101382. [CrossRef]
41. Reynaud, Y.; Lopez, M.; Riaublanc, A.; Souchon, I.; Dupont, D. Hydrolysis of Plant Proteins at the Molecular and Supra-Molecular Scales during in vitro Digestion. *Food Res. Int.* **2020**, *134*, 109204. [CrossRef] [PubMed]
42. Zhu, X.; Wang, L.; Zhang, Z.; Ding, L.; Hang, S. Combination of Fiber-Degrading Enzymatic Hydrolysis and *Lactobacilli* Fermentation Enhances Utilization of Fiber and Protein in Rapeseed Meal as Revealed in Simulated Pig Digestion and Fermentation in vitro. *Anim. Feed Sci. Technol.* **2021**, *278*, 115001. [CrossRef]